

Graphical representation of Salter determinants

This article has been downloaded from IOPscience. Please scroll down to see the full text article.

1985 J. Phys. A: Math. Gen. 18 3283

(<http://iopscience.iop.org/0305-4470/18/17/010>)

View [the table of contents for this issue](#), or go to the [journal homepage](#) for more

Download details:

IP Address: 129.252.86.83

The article was downloaded on 31/05/2010 at 09:16

Please note that [terms and conditions apply](#).

Graphical representation of Slater determinants

W Duch†

Institute of Physics, Quantum Chemistry Group, Nicholas Copernicus University, ul.,
Grudziadzka 5, 87-100 Toruń, Poland

Received 10 April 1985

Abstract. Methods for a graphical representation of determinants are described in detail. Three different graphs are discussed and in each case an efficient graphical method of matrix element evaluation is given. The graphs store information about large determinantal basis sets in a very compact form and allow for some insight into the structure of such basis sets. A computer representation and some algorithms for the graphs are described in the appendices.

1. Introduction

In many branches of physics and theoretical chemistry the Schrödinger equation is solved in some finite-dimensional model space of N -electron functions. Methods that start from the orbital approximation are the most common. Many-electron antisymmetric wavefunctions are then usually represented as a linear combination of Slater determinants, although other choices, such as the use of Gelfand states (Paldus 1976, Shavitt 1983) or spin-adapted antisymmetrised products (Karwowski 1973, Duch and Karwowski 1982), are becoming increasingly popular. Slater determinants, forming a basis of the model space in which solutions of the Schrödinger equation are sought, have to be classified and matrix elements between these determinants, required by the method of solution employed, have to be calculated.

It is the purpose of this paper to show how to describe large sets of determinants with the help of small graphs, how to visualise the structure of model spaces and how to calculate matrix elements using this graphical representation. In the next section the simplest two-slope graphical representation is presented and all the concepts and terminology introduced. This is followed by a section describing an application of the two-slope graph in matrix element calculations. This simple graph has one disadvantage: it describes determinants with different projections of a total spin quantum number M . Because functions with a fixed M number are desired in most methods two alternative graph forms are described and analysed in the subsequent sections, both corresponding to model spaces with a fixed M . The first of these graphs, the three-slope graph, describes orbital configurations, the distribution of α and β spin functions to form a spin-orbital configuration being described by a small, separate diagram. The second graph contains in itself the complete information and is therefore more complex: it has four slopes. However, some parts of these graphs are so simple that an explicit use of their structure becomes very efficient, as shown in § 7. Finally,

† Present address: Max-Planck-Institut für Astrophysik, Karl-Schwarzschild Strasse 1, 8046 Garching bei München, West Germany.

after a brief summary two appendices describe the computer representation of a graph and some useful algorithms for searching the paths in a graph.

It should be emphasised that graphical representation of Gelfand states or, more properly speaking, graphical representation of the so-called 'distinct row table', used by Shavitt, is very similar to the four-slope graph presented here (Shavitt 1977a, 1978, 1983), the only difference coming from the fact that the intermediate M number for determinants may be negative while the intermediate spin quantum numbers S for Gelfand states are always positive. Many concepts related to the graphical representation, as well as the terminology used, are therefore taken from Shavitt. However, Shavitt's graph is usually presented in the context of the unitary group approach (Pladus 1976), the theory requiring much greater effort to understand than the simple considerations presented below. Recently the graphical representation of model spaces encountered in atomic and molecular physics calculations was developed into a general framework (Duch 1985), giving essentially the same results as the group-theoretical approaches by a simpler means. Some results obtained in this framework for determinants are presented here.

2. Classification of determinants—the simplest approach

In this section the idea and all concepts relevant to a graphical representation of N -electron determinantal basis sets are introduced. Determinants are built from spin orbitals which are designated in a standard way: φ_i for spin α and $\bar{\varphi}_i$ for β . A pair $\varphi_i\bar{\varphi}_i$ appearing in a determinant is called a double, unpaired spin orbitals are called singles or singly occupied. For example, the ground state of water may be approximated by a determinant composed of five doubles: $|1a_1\bar{1}a_12a_1\bar{2}a_11b_2\bar{1}b_23a_1\bar{3}a_11b_1\bar{1}b_1|$. Taking this as a reference determinant we may specify excited determinants by writing occupied spin orbitals and their replacements, unoccupied in this reference, for example $(\bar{1}b_23a_1 \rightarrow 4a_1\bar{2}b_2)$. As long as there is only one reference determinant and only single or double replacements are allowed it is easy to store the labels in such a form. However, things get more complicated for higher replacements and several reference determinants.

A good and quite general method of labelling the determinants is to fix a sequence of spin orbitals—for example, according to the increasing orbital energies—and label a determinant by giving occupation numbers for all $2n$ spin orbitals. The determinant label is, in such a case, a bit pattern $110110010\dots$ with bits $2k-1, 2k$ telling us whether spin orbitals $\varphi_k, \bar{\varphi}_k$ are occupied in this determinant or not. One or two computer words are usually enough to store such a spin-orbital configuration. However, if a large number of determinants are used in a calculation the number of words used to store the labels is substantial. Moreover, although such a representation is completely general it does not give us much insight into the structure of our model space; for example, trying to find all determinants interacting (i.e. having non-zero matrix elements) with a given one requires matching it with all the others.

The bit patterns, or spin-orbital occupations, are represented in a convenient way on a grid. The first bit is 0 or 1, 0 represented by a short vertical line (arc) and 1 represented by a skew line. Drawing our bit patterns for a number of determinants we end up with a graph of the kind shown in figure 1.

A path, which is a collection of $2n$ arcs through which one has to pass going from the top of the graph (head of the graph) to the bottom (tail of the graph), is equivalent

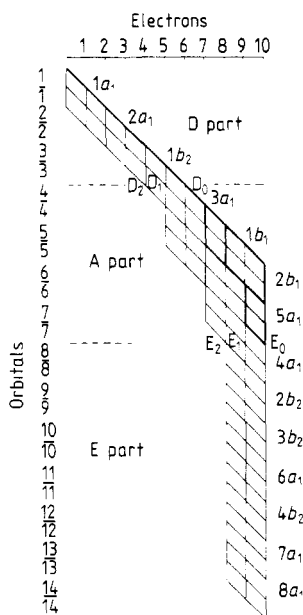


Figure 1. An example of a two-slope graph for 10 electrons and 14 orbitals (double-zeta basis for H₂O). Paths corresponding to the three reference determinants: $|1a_1^2 2a_1^2 1b_2^2 3a_1^2 1b_1^2|$, $|1a_1^2 2a_1^2 1b_2^2 3a_1^2 2b_1^2|$ and $|1a_1^2 2a_1^2 1b_2^2 3a_1 \overline{1b_1} \overline{2b_1} \overline{5a_1}|$ are drawn in bold lines.

to the bit pattern specifying the spin-orbital configuration. The points where the arcs connect are called vertices. It is obvious that all the paths reaching a given vertex v_{ij} (shifted down i units and to the right j units) and coming from the head of the graph form a subgraph corresponding to j electrons distributed among i spin orbitals. Therefore the horizontal axis represents the number of electrons (or cumulative occupation) and the vertical axis the number of spin orbitals. A graph drawn in such a way has a shape that depends on the ordering of spin orbitals. Only in the case of a full space, when all possible determinants that can be formed from a given set of $2n$ spin orbitals are taken as a basis, does the shape not depend on the spin-orbital sequence. In a more common case the many-electron basis (model space) is selected by making single, double or higher replacements of the spin orbitals in some selected reference determinants. Because the graph gives a global description of the determinantal basis set some paths in the graph may correspond to determinants that should not be included. One may choose the ordering of spin orbitals to keep the number of those unwanted paths in the graph to a minimum. Such ordering giving a minimal size of the graph, is achieved by placing at the top all those spin orbitals that appear as doubles in all reference determinants. These spin orbitals will be called d-type and the corresponding part of the graph the D part. A number of singly occupied spin orbitals appear in the reference determinants. These will be called active orbitals or a-type and the corresponding part of the graph the A part. The a- and d-types together are called internal spin orbitals and we have the internal part of the graph or the I part. Finally, orbitals that do not appear in any of the references are called virtual or external or e-type and the corresponding part of the graph the E part.

Looking at figure 1, where single and double excitations from a set of three reference determinants are presented, we can easily recognise these parts by their characteristic

shapes. First we have the D part: an 'arm' formed by single and double excitations from d-type spin orbitals. At each level only three vertices are present because—in the case of double excitations—excited paths differ at most by two arcs from the reference paths, which are in this part represented by the rightmost line. Next comes a complicated, but usually rather small, A part. The reference paths are by definition occupied by all N electrons in the internal part. Therefore in the A part they have to reach the rightmost vertical path going to the tail of the graph. The external part again has a very simple structure, determined by the excitation level. In general, if the excitation level is k , excited paths must not differ from the reference paths by more than $2k$ arcs, i.e. to draw a shape of the graph one has to draw reference paths and, at each level, add k vertices to the left and to the right of each vertex crossed by the reference paths (of course, the number of electrons at each added vertex must stay between 0 and N). The vertices connecting internal and external parts are called E_0, E_1, E_2, \dots , depending on the number of electrons in the external part. The vertices connecting the D and A parts are called D_0, D_1, D_2, \dots , depending on the level of excitation of the internal paths in the D part. Because the structure of the D and E parts is always as simple as in the one reference case one can use this structure explicitly, representing graphically only the A part which bears all the complexity.

Let us now ask: what can the graph be used for? Instead of a list of labels identifying determinants we can have a description of the graph that is much more compact. The graph shown in figure 1 has only 90 vertices and can be fully specified by less than 300 numbers—and even that could be reduced by using the structure of D and E parts in an explicit way—but it describes 92 966 determinants. We may develop some intuitions connected with the shape of the graph, for example, in the configuration-interaction method (Shavitt 1977b) one can estimate how 'good' our model space is, depending on the shape (Duch 1985). We will not explore this topic here because it depends on the particular method we want to work with. A compact description and visualisation of the corresponding structure of the model space are not the only advantages: computational efficiency comes next. Comparing the paths we can easily find the matrix element between corresponding determinants. However, first we will need a numbering scheme for the paths, a mapping of the bit patterns into natural numbers.

Let us consider the vertex v_{ij} , corresponding to i spin orbitals and j electrons. How many paths reach this vertex from the head of the graph? This number, designated w_{ij} and called the weight of a vertex, is obviously equal to the sum of weights of the vertices at level $i-1$ joined with v_{ij} . In our case each vertex is reached from one or two vertices belonging to the level above it. It is very easy to calculate the weights starting from the head (vertex v_{00} with weight fixed as 1) and proceeding to the tail (vertex v_{2nN}) of the graph (figure 2(a)). The weight of the tail is equal to the total number of paths contained in the graph; in the same way the weight of a given vertex v_{ij} is equal to the number of paths in a subgraph which has v_{ij} as its tail, has the same head and is embedded in the main graph.

We could ask: how many j -electron determinants built from the first i spin orbitals are contained in our basis? It is quite easy to calculate if we know how many paths are contained in a subgraph with v_{ij} as its head. This number, designated \bar{w}_{ij} , is simply the weight of a vertex calculated from a reversed graph, i.e. with the tail as its head (figure 2(b)). Multiplying $w_{ij}\bar{w}_{ij}$ we find the number of determinants with j electrons occupying the first group of i spin orbitals and $N-j$ electrons occupying $2n-i$ spin orbitals.

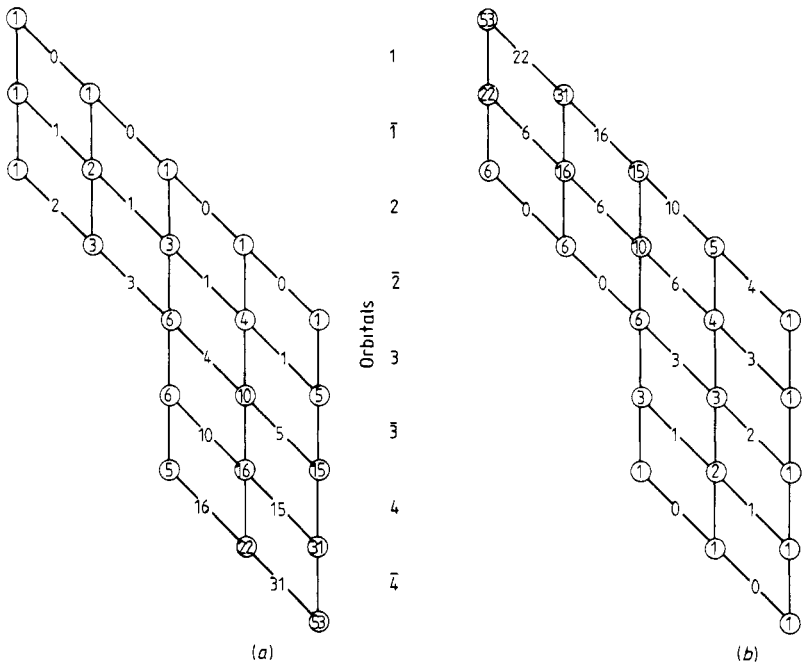


Figure 2. Lexical (a) and reverse lexical (b) labelling of the vertices in a two-slope graph. The weight of an empty arc is always zero. The sum of the arc weights gives a lexical (reverse lexical) index of a path.

Using the weights we can easily calculate, in a systematic way, a position of a given path among other paths of the graph. We will assign the weights to the arcs in such a way that the position of the path—called its lexical index and designated by m_L , where L represents spin-orbit configurations—is given as a sum of the $2n$ arc weights for that path. Let the weight of an empty (vertical) arc always be zero. How to assign a weight to a skew arc? Let us imagine two paths, joined at some vertex v_{ij} and identical below the i th level. We want the paths joining v_{ij} through a skew arc to have higher lexical indices than those joining it through an empty arc. To assure this let us assign the number of paths coming through an empty arc, i.e. w_{i-1j} , as the weight of an arc joining v_{ij} with v_{i-1j-1} (figure 2(a)). The highest contribution to m_L from the paths coming through an empty arc is equal to w_{i-1j-1} , while those coming through the skew arc contribute at least w_{i-1j} . This indexing scheme works not only for the whole graph. For each subgraph with the same head and v_{ij} as its tail we obtain lexical indices from 0 to $w_{ij} - 1$, with the highest (rightmost) path as 0 and the lowest (leftmost) path as $w_{ij} - 1$.

Some of the paths which are in the graph, even if it has minimal shape, may not correspond to the determinants we would like to use, either because they have the wrong symmetry or the level of excitation is higher than desired. The symmetry of the determinant is, in the case of point groups with one-dimensional representations, a product of the representations of the singly occupied orbitals. Treatment of degenerate representations of symmetry groups requires a combination of determinants and is beyond the scope of this paper.

One can develop different schemes to remove unwanted paths by adding more dimensions (cf § 4) to our graph, splitting the vertices, adding excitation level indices

to each vertex or complicating the graph in some other way, but the simplest and most flexible way to dispose of them without changing the graph itself is to introduce a double-level indexing scheme: the address of a given path with lexical index m_L is stored as an entry in a vector—called the index vector—at position m_L , i.e. $I(m_L)$ is the desired position of the spin-orbital configuration (function) L among other basis functions. In this way not only can we delete configurations, but also we can reorder them arbitrarily, for example according to the symmetry species in the internal part of the graph.

3. Calculation of matrix elements using spin-orbital (two-slope) graph

Using the graph and the indexing scheme described above we will find a matrix representation of the Hamiltonian in the model space described by the graph. Matrix elements of other types of operators are calculated in an analogous way. Any k -particle operator acting in our model space can be expressed as a combination of creation and annihilation operators, or as products of k 'replacement' operators

$$E_{i\sigma, j\tau} = a_{i\sigma}^+ a_{j\tau} = \sum_{p=1}^N |\varphi_i(\nu_p)\sigma(\vartheta_p)\rangle \langle \varphi_j(\nu_p)\tau(\vartheta_p)| \quad (1)$$

replacing the spin orbital $\varphi_j\tau$ by $\varphi_i\sigma$ or, in the graph's path, segment $(j\tau)$ by segment $(i\sigma)$.

We are concerned not so much with the method of matrix element calculation—Slater rules in this case—but rather with the whole organisation of the computation. The straightforward approach—checking each determinant against all the others in the list—is very inefficient. Using the graph we immediately see all paths (determinants) interacting with a given one: for two-particle operators interacting determinants can differ at most by two spin orbitals, i.e. $2n-4$ spin-orbital occupations should be identical. The two interacting paths have therefore at most four arcs that are not parallel, branching into empty and singly occupied arcs first and joining by singly occupied and an empty arc a number of levels below, thus forming a loop in the graph (figure 3). The non-parallel arcs of the two paths involved in a loop are called the loop segments. In the case of a four-segment loop only three different shapes are possible, and for the two-segment loop (determinants differing by one orbital) obviously only one shape is possible. For k -particle operators more than $2k$ -segment loops give vanishing matrix elements. Because each loop must contain the same number of expanding segments (increasing the distance between the paths) as contracting segments (decreasing this distance) the number of segments is always even. Using Slater rules (Slater 1968) we can easily calculate matrix elements for the three types of four-segment loops and for one type of a two-segment loop, as shown in figure 3. The path, designated by L in figure 3, always has a higher lexical index than the one designated by R. Thus the loops give a contribution to the lower triangle of the \mathbf{H} matrix. Two distinct approaches may be taken to calculate the whole \mathbf{H} matrix. First, we can fix one of the paths, say L, and create all the interacting loops, thus calculating a row of the matrix. This 'matrix element driven' approach requires an easy access to the integrals. The second approach starts from the integrals and therefore may be called 'integral driven' (cf Saunders and van Lenthe 1983). The integral labels $i < j < k < l$ (or $i < j$

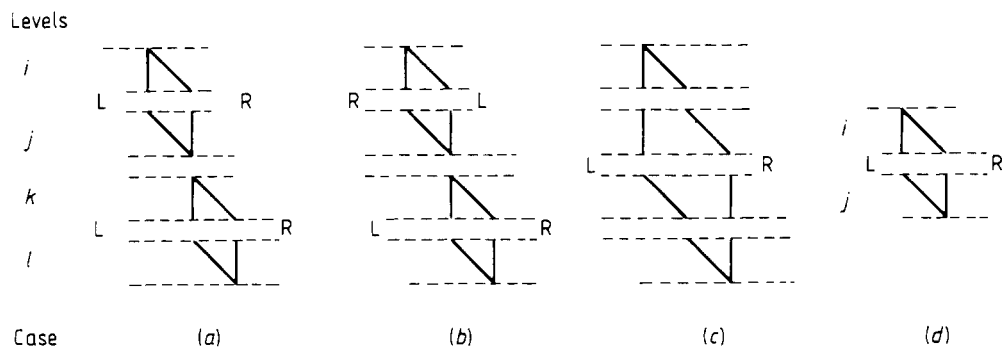


Figure 3. Possible kinds of loops in a two-slope graph. The formulae for matrix elements $\langle L|H|R \rangle$ in cases (a), (b), (c) of the four-segments loops are:

$$\begin{aligned}
 (a) \quad \langle L|H|R \rangle &= \varepsilon_{LR} \{ (ij \| kl) - (il \| jk) \} \\
 (b) \quad \langle L|H|R \rangle &= \varepsilon_{LR} \{ (ij \| kl) - (ik \| jl) \} \\
 (c) \quad \langle L|H|R \rangle &= \varepsilon_{LR} \{ (ik \| jl) - (il \| jk) \}
 \end{aligned}
 \quad \varepsilon_{LR} (-1)^{\bar{i} + \bar{j} + \bar{k} + \bar{l}}$$

where $(ij \| kl) = \delta(\theta_i, \theta_j) \phi(\theta_k, \theta_l) (ij \| kl)$ includes integration over the spin functions and \bar{i} is the number of occupied spin orbitals (the N coordinate in the graph) in the path in which orbital i is occupied. The two-segment loop (d) corresponds to matrix element:

$$(d) \quad \langle L|H|R \rangle = (-1)^{\bar{i} + \bar{j}} \left((i \| j) + \sum_{k \neq i, j} [(ij \| kk) - (ik \| jk)] \right)$$

where $(i \| j) = (i | j) \delta(\theta_i, \theta_j)$.

for one-electron integrals) fix the levels of the graph where the loop segments are placed. For the three loop shapes shown in figure 3 three unique values of the matrix elements are found, using combinations of $(ij | kl)$ integrals. Each value of the matrix element appears in many places in the \mathbf{H} matrix, as shown in figure 4. This allows for a compact representation of the matrix, with one value of matrix element and a series of addresses where this element appears.

In some methods we may avoid construction of large matrices (like the \mathbf{H} matrix in our model space), using the philosophy of the direct configuration-interaction method (Roos 1972, Roos and Siegbahn 1977) or the vector method (Hausman and Bender 1977), especially if the \mathbf{E} part of the graph is relatively large and simple.

At this point we know how to construct the graph (the computer representation is described in appendix 1), how to calculate lexical indices of the paths and how to remove unwanted paths, how to form loops and calculate matrix elements. We have defined the language useful for different graphical representations of many-particle model spaces. Leaving aside details of the computational methods that may benefit from the use of the graph (details easily elaborated on for particular applications), we will try to improve the graph itself. The efficiency of the graphical representation depends on the number of paths deleted. The graph described so far has no restrictions on the M quantum number, thus describing determinants with all possible projections of total spin. Although such graphs are of some use (Esser 1984) the number of unwanted paths is too high to be able to remove them efficiently with the help of an index vector (many loops created in the graph have to be discarded because one of the paths has the wrong M). Therefore a modification of the graph to describe model spaces with fixed M number is desired.

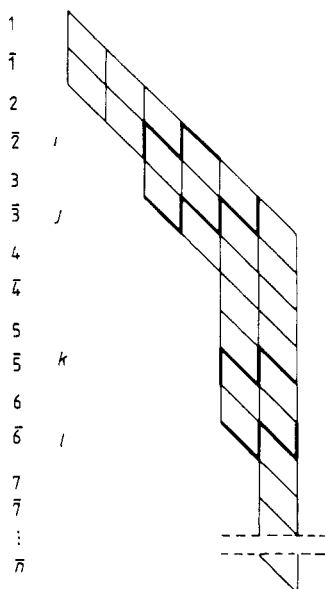


Figure 4. Example of four-segment loops giving the same value of matrix element, the value uniquely determined by the i, j, k, l levels where non-parallel loop segments (drawn with bold lines) are placed. It does not depend on the connections between the segments (except for a sign change).

4. Improved graphs for determinants

Looking at the graph in figure 1 one is first tempted to place all the orbitals with spin β at the bottom with spin α orbitals at the top. We will obtain in this way two graphs joined by one vertex, containing the paths with fixed number of α - and β -type spin orbitals, i.e. fixed M (figure 5). However, it is not possible to draw this graph in such a way that automatically excludes a large number of paths being excited higher than specified. If k -fold excitation is desired and in the α part of the graph l -fold excitation was performed, the $(k-l)$ -fold excited β graph should be attached to it. Additional complications arise with explicit separation of the E part and with an indexing of the paths. Such an approach is not elegant enough and although it may be computationally useful (Wasilewski 1984) it is not elaborated on here.

We will follow another route instead. We have used an excited configuration of water, $(\overline{1b_2}3a_1 \rightarrow 4a_1\overline{2b_2}) = |1a_1\overline{1a_1}2a_2\overline{2a_2}1b_24a_1\overline{2b_2}3\overline{a_1}1b_1\overline{1b_1}|$. Let us now ask: how many different determinants can we build from the same orbitals by permuting all α and β spin functions? In other words: how many spin-orbital configurations can we associate with a given orbital configuration? Obviously, changing spin distribution among doubles we get either zero (if the two identical orbitals appear with the same spin function, like in $|1a_1\overline{1a_1}2a_1\overline{2a_1} \dots|$) or a change of sign (if we change the order within doubles, like in $|\overline{1a_1}1a_1 \dots|$). Therefore it is enough to consider permutations of spin functions among singles only. How do we classify determinants associated with the same orbital configuration? In our example, omitting doubles we have four spin functions, two of α and two of β type. A simple graphical way to classify them (Pauncz 1979) is shown in figure 6. The horizontal axis shows the value of the projection

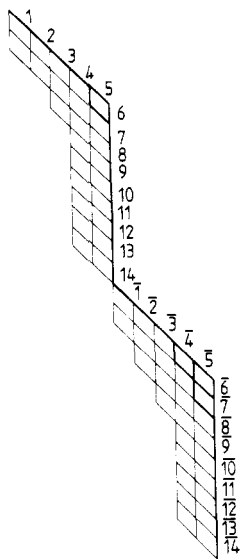


Figure 5. The graph of figure 1 with α - and β -type spin orbitals separated.

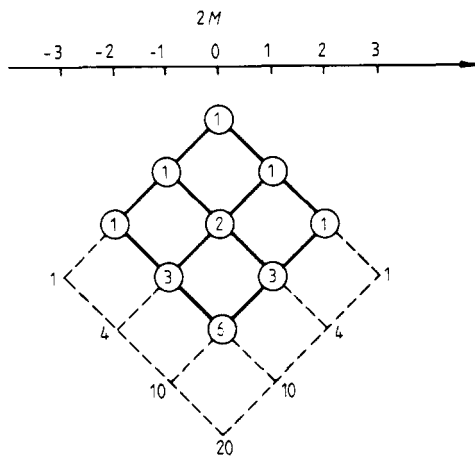


Figure 6. Example of the M diagram classifying distribution of the α and β spin functions among singly occupied orbitals of a configuration with $M = 0$ containing four singles (full lines) or six singles (broken lines).

of spin, i.e. M number, and the vertical axis the number of spin functions. This type of graph, topologically equivalent to spin-orbital graphs described in the previous section, will be called the M diagram. Each path in the M diagram represents a certain distribution of spin functions α and β among singly occupied orbitals, for example the rightmost path corresponds to $|\dots 1\bar{b}_2 3a_1 4a_2 \bar{2}b_2 \dots|$ and the leftmost to $|\dots \bar{1}b_2 3a_1 4a_2 2b_2 \dots|$.

We want to expand this picture to include all n orbitals, and also the unoccupied and doubly occupied ones. Two things should be represented: the number of electrons as a function of the number of orbitals, as shown before in figure 1, and the intermediate

M values, as shown in figure 6. Straightforward generalisation of these two graphs leads to a three-dimensional structure, shown from the front and from the side in figure 7, where four electrons are distributed in six orbitals. Looking at the graph from the front we cannot distinguish between empty and doubly occupied orbitals, because they contribute nothing to the M values. Looking from the side we cannot see the difference between α - and β -type orbitals. Two consecutive singles, one of α and one of β type, do not change the value of M and may be replaced by an empty and a doubly occupied orbital (occupations 0,2 or 2,0), as shown in figure 6(b). Notice that now the graph has only n levels, not $2n$ as before. The projections are quite easy to draw, and although we do not draw the three-dimensional graph itself, one can represent it in a rather straightforward way on a computer. However, computational efficiency should not be the only reason to use the graph. Equally important is a visualisation, an insight into the structure of the model space.

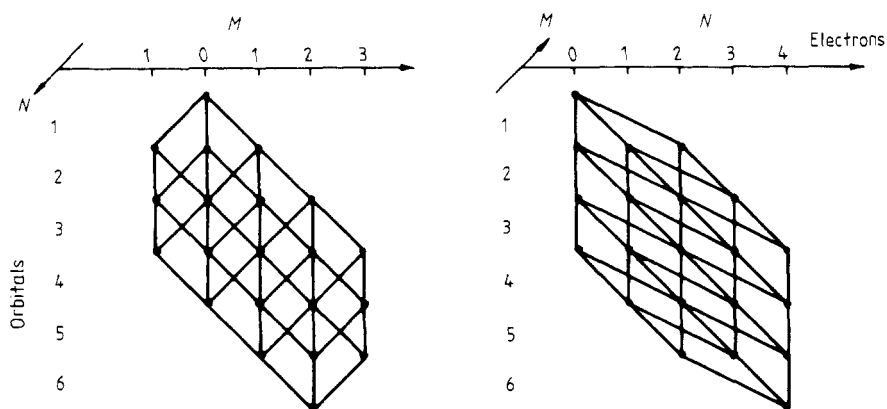


Figure 7. Two perpendicular projections of a three-dimensional graph.

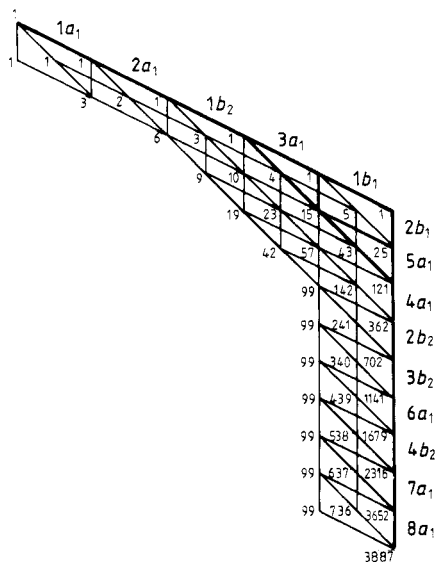
(a) Front view. The M axis lies in the plane of the drawing and the N axis is perpendicular to this plane. Vertical lines represent empty or doubly occupied orbitals (no difference is seen from this direction), lines with decreasing M represent β -type singles, lines with increasing M represent α -type singles.

(b) Side view. The M axis is now perpendicular to the plane; no difference is seen between the α - and β -type singles.

Looking closer at figure 7 we find that the side projection contains physically more relevant information. It describes our model space in terms of the orbital configurations. Groups of determinants associated with each configuration are ordered by means of the M diagram. The arcs of the orbital configuration graphs have three slopes (occupations 0, 1 and 2) which makes its structure considerably more complicated than a simple two-slope graph. In figure 8 the graph of figure 1 is represented as the graph of orbital configurations. Although the structure of the three-slope graph is more complicated it is smaller than its two-slope version. It has n rows instead of $2n$ rows and contains fewer unwanted paths. Each path is connected with a group of

$$d(M, s) = \binom{s}{s/2 + M}$$

determinants, where s is the number of singles in the path.



The one- and two-electron integrals are defined as

$$\begin{aligned}(i|j) &= \int \varphi_i^*(1) \hat{h}_1(1) \varphi_j(1) dV_1 \\(ij|kl) &= \int \varphi_i^*(1) \varphi_k^*(2) \hat{h}_2(1, 2) \varphi_j(1) \varphi_l(2) dV_1 dV_2 \\J_{ij} &= (ii|jj) \quad K_{ij} = (ij|ij).\end{aligned}\tag{3}$$

We can distinguish three cases: L = R, L and R differ by one orbital, and L differs from R by two orbitals. Each case is treated separately.

5.1. Identical configurations

The formula in this case contains a strictly diagonal part, as well as the rest of the $d(M, s_L)$ by $d(M, s_L)$ matrix. The off-diagonal elements, when shown as loops in the two-slope graph, correspond to cases (a) and (b) in figure 3, with $\varphi_j = \bar{\varphi}_i$ and $\varphi_l = \bar{\varphi}_k$. Because the orbitals are the same, only the spin functions differ. The paths do not split in the three-slope graph, but they split in the M diagram (figure 6). The formula has a scalar part, common to all diagonal elements, and a matrix part \mathbf{K} :

$$\langle L|H|L \rangle = \left(\sum_{i=1}^n n_i (i|i) + \sum_{i,j=1}^n \delta_{n,2} (\delta_{n,1} + \delta_{n,2}) (2J_{ij} - K_{ij}) + \sum_{i < j} \delta_{n,1} \delta_{n,1} J_{ij} \right) \mathbf{I} - \mathbf{K}\tag{4}$$

where \mathbf{I} is the unit matrix and \mathbf{K} is a symmetric matrix of exchange integrals. Let us designate by \bar{i} the position of orbital i among singles (e.g. if $L = 222111000$, for $i = 5$ we have $\bar{i} = 2$). The K_{ij} integral is added to the K_{lm} element if, exchanging segments i with j in the M -diagram path number m , path number l is obtained. To calculate the m th row (or column) we act on the M -diagram path $|m\rangle$, starting with $\bar{i} = 1$, $\bar{j} = 2, 3, \dots, s_L$ to $\bar{i} = s_L - 1$, $\bar{j} = s_L$, each time adding K_{ij} to the column (row) $|l\rangle = (\bar{i}, \bar{j})|m\rangle$. For example, for the configuration $L = 222111000$ row $|1\rangle = |++--\rangle$, where $+$ stands for α and $-$ for β type arc in the M diagram, the following six elements are created in the first row and column of the \mathbf{K} matrix: $(K_{45} + K_{67}, K_{56}, K_{46}, K_{57}, K_{47}, 0)$.

It is easy to organise the computation of diagonal matrix elements in such a way that only a small part of the formula has to be recomputed each time the path L is changed.

5.2. One orbital difference

There are $N - 1$ identically occupied spin orbitals in the two determinants involved in the matrix element. Let us designate by i and j , $i < j$, the orbital which is different in R and L . In the three-slope graph the two paths are identical between the head and the level $i - 1$. At the level i they diverge; a segment of a loop that is formed has occupations $|0\ 1\rangle$ or $|1\ 2\rangle$. The paths run parallel down to the level $j - 1$ and at the level j are closed by the $|1\ 0\rangle$ or $|2\ 1\rangle$ segment. Thus four different two-segment loop structures are possible (figure 7): $\begin{bmatrix} 0 & 1 \\ 1 & 0 \end{bmatrix}$, $\begin{bmatrix} 0 & 1 \\ 2 & 1 \end{bmatrix}$, $\begin{bmatrix} 1 & 2 \\ 1 & 0 \end{bmatrix}$ and $\begin{bmatrix} 1 & 2 \\ 2 & 1 \end{bmatrix}$, the upper segment belonging to the level i , lower to j . In each case orbital j has greater occupation in the L (left) path, the path with a higher lexical index than the R (right) path.

We should place orbital i at the same position as j , so that identical spin orbitals will occupy the same $N - 1$ positions in L as in R . We can shift orbitals in one of the

configurations, applying a cyclic permutation, but it is simpler to shift i and j orbitals to the first first position of both L and R. The four cases mentioned above lead to the following types of elements: $\langle j\dots|H|i\dots\rangle$, $\langle jj\dots|H|ij, ,\rangle$, $\langle ij\dots|H|ii\dots\rangle$ and $\langle ij\dots|H|ij\dots\rangle$. For simplicity spin labels are omitted here; orbitals at the same positions must have the same spin functions, otherwise the element is zero. The phase factor coming from the shift of columns in the corresponding determinants is equal to $(-1)^{\bar{i}+\bar{j}}\epsilon_w$, where ϵ_w depends on the loop structure. In the first case $\epsilon_w = 1$. In the second case, shifting of the jj pair may introduce a change of sign only if the α, β order of spin orbitals is reversed inside the pair—this ‘inner’ parity is designated further by ϵ_j —and shifting of i and j in R introduces $-(-1)^{\bar{i}+\bar{j}}$, so that $\epsilon_w = -\epsilon_j$. In the third case we have $\epsilon_w = -\epsilon_i$ similarly. The fourth case gives $\epsilon_w = -1$ because the second orbital— j in L and i in R—must have the same spin function in both determinants, so that the inner parity of ii and jj has to be opposite and, as a result, $\epsilon_i\epsilon_j = -1$.

Calculation of the phase factors may also easily be done segment-wise: segments of the type $|0\ 1|$ or $|1\ 0|$ always contribute $+1$, while those of the type $|1\ 2|$ and $|2\ 1|$ contribute $-\epsilon_p$, where p is the level at which these segments are placed. The $(-1)^{\bar{i}+\bar{j}}$ factor replaces the need to count segments other than i and j . We can now write the formula for a block of matrix elements associated with the two orbital configurations:

$$\langle L|H|R\rangle = (-1)^{\bar{i}+\bar{j}} \left[\left((i|j) + \sum_{k=1}^n (n_k(ij|kk) - \delta_{n_k,2}(ik|jk)) \right) \mathbf{I}_{LR} - \mathbf{K}_{LR} \right] \tag{5}$$

where $n_k = \min(n_k^L, n_k^R)$ and the non-zero elements of $d(M, s_L)$ by $d(M, s_R)$ matrices \mathbf{I}_{LR} and \mathbf{K}_{LR} are defined as

$$l = \mathcal{L}(\hat{P}_L f) \quad r = \mathcal{L}(\hat{P}_R f)$$

$$\mathbf{I}_{LR}(l, r) = \epsilon_w \quad \mathbf{K}_{LR}(l, r) = \epsilon_w \sum_{\substack{k=1 \\ k \neq i, j}}^n \delta_{n_k,1} \delta(\epsilon_j, \theta_k)(ik|jk) \tag{6}$$

where f is one of the M -diagram paths, identical for L and R, corresponding to the singles in the configurations with all i and j orbitals shifted to the first positions; \hat{P}_L and \hat{P}_R simply shift i and j back to their original positions \bar{i} and \bar{j} in L and R: $\mathcal{L}(f')$ gives a lexical index of the M -diagram path f' , and $\delta(\theta_j, \theta_k)$ vanishes unless the spin function θ_k of orbital k is the same as θ_j , where j is the ‘different’ orbital in L placed against i in R.

As an example let us calculate the \mathbf{I}_{LR} and \mathbf{K}_{LR} matrices for $L = 222111100$ and $R = 222121000$. Comparing the two occupation patterns we find the loop structure $\begin{vmatrix} 1 & 2 \\ i & j \end{vmatrix}$ with $i = 5, j = 7$ and $\bar{i} = 2, \bar{j} = 4$. The transformed element $\langle L|H|R\rangle = \langle ij\dots|H|ii\dots\rangle$ has $(-1)^{\bar{i}+\bar{j}} = +1$ and $\epsilon_w = -\epsilon_i$. There are four common M -diagram paths f possible in this case: rows l are obtained by shifting i, j from the first and second position to $\bar{i} = 2, \bar{j} = 4$ in L and columns r by dropping the first two symbols in the f path. Using the M diagram we can easily convert the path’s symbols into numbers:

$$\begin{array}{c} \text{R: } i \quad i \\ \text{L: } i \quad j \quad 4 \quad 6 \\ \epsilon_w: -1 \begin{bmatrix} + & - & + & - \\ + & - & - & + \\ - & + & + & - \\ - & + & - & + \end{bmatrix} \end{array} \xrightarrow[\bar{j}=4]{\text{L: } \bar{i}=2} \mathcal{L} \begin{array}{c} \begin{bmatrix} 4 & i & 6 & j \\ + & + & - & - \\ - & + & + & - \\ + & - & - & + \\ - & - & + & + \end{bmatrix} = \begin{bmatrix} 1 \\ 3 \\ 4 \\ 6 \end{bmatrix} \end{array}$$

$$\xrightarrow{R:} \mathcal{L} \begin{matrix} & 4 & 6 \\ + & - \\ - & + \\ + & - \\ - & + \end{matrix} = \begin{bmatrix} 1 \\ 2 \\ 1 \\ 2 \end{bmatrix}$$

$$I_{LR} = \begin{bmatrix} -1 & 0 \\ 0 & 0 \\ 0 & -1 \\ 1 & 0 \\ 0 & 0 \\ 0 & 1 \end{bmatrix} \quad K_{LR} = \begin{bmatrix} -(i6|6j) & 0 \\ 0 & 0 \\ 0 & -(i4|4j) \\ (i4|4j) & 0 \\ 0 & 0 \\ 0 & (i6|6j) \end{bmatrix}.$$

No more than two non-zero entries in each column (or row) are possible for matrix elements between configurations differing by one orbital.

5.3. Two orbitals different

Three subcases exist here, corresponding to loops with two, three or four segments.

(i) Two-segment loops: the two determinants differ by one pair of orbitals, so that

$$\langle L|H|R\rangle = \langle jj \dots |H|ii \dots \rangle = (ij|ij)I \tag{7}$$

where I is a $d(M, s_L)$ -dimensional unit matrix. In the graph the loop structure is $\begin{bmatrix} 0 & 2 \\ 2 & 0 \end{bmatrix}$.

(ii) Three-segment loops: one of the two configurations contains a double which is not present in the other, i.e. a segment $|0\ 2\rangle$ or $|2\ 0\rangle$ appears. As usual, configuration L is the one with greater lexical index. Suppose that $|0\ 2\rangle$ is the highest segment of our loop structure. Each of the two segments needed to complete the three-segment loop is of $|1\ 0\rangle$ or $|2\ 1\rangle$ type, giving four different structures. The segment $|0\ 2\rangle$ may also appear in the middle, giving another four structures. However, putting this segment as the lowest would make the lexical index of L lower than that of R . Therefore $|2\ 0\rangle$ should be taken as the bottom segment, and consequently the other segments are $|0\ 1\rangle$ or $|1\ 2\rangle$. Thus a total of 12 different loop structures are possible in this case. Let us designate the orbital corresponding to the $|0\ 2\rangle$ or $|2\ 0\rangle$ level as d and the remaining two p and q , $p < q$. The formula is then:

$$\langle L|H|R\rangle = -(-1)^{\bar{p}+\bar{q}}(pd|qd)I_{LR} \tag{8}$$

$$I_{LR}(l, r) = \begin{cases} 1 & \text{if one } |0\ 1\rangle \text{ or } |1\ 0\rangle \text{ segment is present} \\ \varepsilon_d & \text{otherwise} \end{cases}$$

with l, r indices defined as in (6).

(ii) Four-segment loops: the four levels are designated $i < j < k < l$. Three different two-electron integrals may be formed in the case of a symmetric operator \hat{h}_2 and real orbitals:

$$J_1 = (ij|kl) \quad J_2 = (il|jk) \quad J_3 = (ik|jl).$$

In § 5.2 we have identified four two-segment loop types, with the phase factors $(-1)^{\bar{i}+\bar{j}}\varepsilon_{w}$. We can combine two-segment loops at levels i, j with the two-segment loops at levels k, l in the two ways, as is shown in figures 3(a) and (b). There are $4 \times 4 = 16$ loop structures in each case and the 'open' loops, like those in figure 3(c), add another 16, so there is a total of 48 loop structures. A different combination of

integrals corresponds to each kind of loop:

$$\langle L|H|R\rangle = \epsilon_{LR}[(ij|kl)I_{LR}^1 - (il|jk)I_{LR}^2] \tag{9a}$$

$$\langle L|H|R\rangle = \epsilon_{LR}[(ij|kl)I_{LR}^1 - (ik|jl)I_{LR}^3] \tag{9b}$$

$$\langle L|H|R\rangle = \epsilon_{LR}[(ik|jl)I_{LR}^3 - (il|jk)I_{LR}^2] \tag{9c}$$

$$\epsilon_{LR} = (-1)^{\bar{i}+\bar{j}+\bar{k}+\bar{l}}$$

where ϵ_{LR} is a common factor due to reordering of orbitals to the first positions in the L and R determinants, and the elements of I_{LR}^p are zero or equal to ϵ_w , the product of inner parities of doubles involved in the loop structure. We may simplify this product noting that $\epsilon_i\epsilon_j = \epsilon_k\epsilon_l = -1$ for I_{LR}^1 , because I_{LR}^1 is multiplied by $(ij|kl)$ integral and, because i and j (or k and l) are both doubles, the second i orbital must have the same spin function as the first j orbital in the opposite determinant, so that $\varphi_i(q)\bar{\varphi}_i(q+1)$ in the first determinant corresponds to $\bar{\varphi}_j(q+1)\varphi_j(q+2)$ in the second, giving $\epsilon_i\epsilon_j = -1$. For I_{LR}^2 matrices the same argument leads to $\epsilon_i\epsilon_l = \epsilon_j\epsilon_k = -1$, and for I_{LR}^3 to $\epsilon_i\epsilon_k = \epsilon_j\epsilon_l = -1$. Thus ϵ_w is a product of all ϵ_d , where d is the level at which the $|2\ 1|$ or $|1\ 2|$ segment is present, with some of the $\epsilon_d\epsilon_{d'} = -1$. Moreover, the single and double arcs joined in one vertex form $|1\ 2|$ or $|2\ 1|$ segments contributing $-\epsilon_d$, while those disjoint contribute $+\epsilon_d$, as shown in table 1.

The non-zero elements of I_{LR}^p matrices, equal to ϵ_w , are determined using the same method as in the previous subsection, i.e. we take a common spin path f , corresponding to the determinants with i, j, k, l orbitals shifted to the first positions and reordered so that i is placed against j for I_{LR}^1 , or against l for I_{LR}^2 , or against k for I_{LR}^3 , and shift the orbitals back to their original i, j, k, l positions. As a result the M -diagram paths are obtained; after removing the symbols corresponding to doubles, lexical indices of the paths are calculated from the M diagram. This procedure is illustrated here by an example:

$$\text{loop: } \begin{array}{c|cc} i & 0 & 1 \\ j & 1 & 2 \\ k & 1 & 0 \\ l & 2 & 1 \end{array} \quad \begin{array}{l} \bar{i}=1 \\ \bar{j}=2 \\ \bar{k}=3 \\ \bar{l}=3 \end{array} \quad \begin{array}{l} s_L = s_R = 4 \\ \epsilon_{LR} = -1 \\ \langle L|H|R\rangle = -(ik|jl)I_{LR}^3 + (il|jk)I_{LR}^2 \end{array}$$

structure of I_{LR}^3 : $\epsilon_w = \epsilon_j(-\epsilon_l) = +1$

$$\begin{array}{l} \text{R: } i \quad j \quad j \quad l \\ \text{L: } k \quad j \quad l \quad l \\ \epsilon_w: 1 \end{array} \begin{bmatrix} + & + & - & + & - & - \\ + & - & + & - & + & - \\ & & & & - & + \\ - & + & - & + & + & - \\ & & & & - & + \\ - & - & + & - & + & + \end{bmatrix} \xrightarrow[\bar{l}=3]{\text{R: } \bar{i}=1} \mathcal{L} \begin{array}{cc} i & l \\ \begin{bmatrix} + & - & + & - \\ + & + & - & - \\ + & - & - & + \\ - & + & + & - \\ - & - & + & + \\ - & + & - & + \end{bmatrix} & = \begin{bmatrix} 2 \\ 1 \\ 4 \\ 3 \\ 6 \\ 5 \end{bmatrix} \end{array}$$

$$\xrightarrow[\bar{k}=3]{\text{L: } \bar{j}=2} \mathcal{L} \begin{array}{cc} j & k \\ \begin{bmatrix} - & + & + & - \\ + & - & + & - \\ - & - & + & + \\ + & + & - & - \\ - & + & - & + \\ + & - & - & + \end{bmatrix} & = \begin{bmatrix} 3 \\ 2 \\ 6 \\ 1 \\ 5 \\ 4 \end{bmatrix} \end{array}$$

$$l_{LR}^3 = [3, 1, 2, 5, 6, 4]$$

structure of l_{LR}^2 : $\epsilon_{\lambda} = -\epsilon_j \epsilon_l$

$$\begin{array}{c}
 \begin{array}{c}
 \text{R: } i \quad j \quad j \quad l \\
 \text{L: } l \quad j \quad k \quad l \\
 \epsilon_w: -1 \\
 \text{common paths} \\
 +1
 \end{array}
 \begin{bmatrix}
 + & + & - & - & + & - \\
 & & & & - & + \\
 - & - & + & + & + & - \\
 + & - & + & - & + & - \\
 - & + & - & + & + & - \\
 & & & & - & +
 \end{bmatrix}
 \xrightarrow[\bar{l}=3]{\text{R: } \bar{i}=1} \mathcal{L}
 \begin{bmatrix}
 + & + & - & - \\
 + & - & - & + \\
 - & + & + & - \\
 - & - & + & + \\
 + & + & - & - \\
 + & - & - & + \\
 - & + & + & - \\
 - & - & + & +
 \end{bmatrix}
 =
 \begin{bmatrix}
 1 \\
 4 \\
 3 \\
 6 \\
 1 \\
 4 \\
 3 \\
 6
 \end{bmatrix} \\
 \\
 \xrightarrow[\bar{k}=3]{\text{L: } \bar{j}=2} \mathcal{L}
 \begin{bmatrix}
 + & + & - & - \\
 - & + & - & + \\
 + & - & + & - \\
 - & - & + & + \\
 + & - & + & - \\
 - & - & + & + \\
 + & + & - & - \\
 - & + & - & +
 \end{bmatrix}
 =
 \begin{bmatrix}
 1 \\
 5 \\
 2 \\
 6 \\
 2 \\
 6 \\
 1 \\
 5
 \end{bmatrix}
 \end{array}$$

$$l_{LR}^2 = -[1, 3, 0, 0, 4, 6] + [3, 1, 0, 0, 6, 4]$$

Table 1. Phase factors for the three-slope graph, two- and four-segment loops. Segments |0 1| or |1 0|: always +1; |0 2| or |2 0|: always $-\epsilon_p$.

$\Delta e(p)$	-2	-1	0	1	2
1 2	-	$+\epsilon_p$	$-\epsilon_p$	$-\epsilon_p$	$+\epsilon_p$
2 1	$+\epsilon_p$	$-\epsilon_p$	$-\epsilon_p$	$+\epsilon_p$	-

The left arc of the segment reaches vertex (p, N_L) , and the right arc reaches vertex (p, N_R) . $\Delta e(p) = N_R - N_L$; ϵ_p is the inner parity of a doubly occupied orbital p , i.e. for \overline{pp} ordering it is +1 and for $\overline{p\overline{p}}$ it is -1.

where the symbol $[1, 3, 0, 0, 4, 6]$ designates a matrix with non-zero elements equal to +1 in column 1, row 1, 3 in row 2, 4 in row 5, 6 in row 6, and zeros everywhere in rows 3 and 4. The number of non-zero elements per column (row) in the l_{LR}^p matrices is, at most, 4, so they can be represented in a compact way. The symbols of the M -diagram paths in R and L are obtained from those of the common paths by reordering and removing the symbols corresponding to doubles. Actually there is no need to create these symbols; it is enough to know the reordering and use the common path symbols to read off the M -diagram arc weights. For example, to get the R paths written above we have to use symbols 1, 5, 4, 6 of the common paths. Although there may be $s_L + 2$ or $s_L + 4$ symbols in a common path, omitting the doubles M diagram for s_L singles is always used.

Matrix elements of the same value (up to a phase) appear for all 16 loop structures corresponding to equation 9(a) (similarly 9(b) or 9(c)), no matter where we place the segments in the graph and how the four loop levels are connected. The structure of I_{LR}^p matrices depends on the positions i, j, k, l , i.e. it is changed only if the number of singles between the loop levels is changed. The graph allows us to find all matrix elements that are equal and thus to use the structure of our model space in the most complete way (figure 4).

The last remark of this section is addressed to those who know some group theory. The matrices I_{LR}^p depend on the permutation placing identical orbitals in L and R against each other. In fact, they form a reducible representation of the permutation group. The reducibility comes from the fact that, for spin-independent operators, not only M , but also S , the total value of the spin, is a good quantum number. Thus six determinants associated with a configuration with four singles are transformed to two singlet, three triplet and one quintet combinations ($2+3+1=6$), or twenty determinants for six singles into five singlets, nine triplets, five quintets and one septet ($5+9+5+1=20$), etc. One can easily find the transformation replacing I_{LR}^p by the matrices corresponding to the desired spin subspace (Duch 1985). However, such considerations would lead us too far from the main subject of this paper.

6. The four-slope graph

There is another way of projecting the three-dimensional graph on a plane: instead of taking exactly perpendicular projections (figures 7 and 8) we will shift our point of view to see the difference between α - and β -type singles. As a result four different arc slopes are seen in the projected graph, depending on the occupation numbers and the spin function types of the orbitals (figure 9). We may choose our point of view in such a way that the arc slope for α -type single (designated by $\bar{1}$) is steeper than the slope for β -type single (designated by 1). Although two consecutive arcs of the type $\bar{1}\bar{1}$ or 11 reach the same vertex as the 02 or 20 arcs, the arcs $\bar{1}\bar{1}$ and 11 do not. Therefore the simple interpretation of the horizontal axis as the number of electrons cannot be preserved. Each vertex has a uniquely specified M' value. For the vertices with $M'=0$ we can draw a horizontal axis with the number of electrons $N'=0, 2, 4, \dots$, while for the adjacent vertices with $M' \neq 0$ the paths reaching them contain $N'+M'$ electrons.

The path in a four-slope graph contains n arcs and describes the spin-orbital configuration. All concepts described in the previous sections for the two-slope and three-slope graphs are immediately extended to the four-slope case. The picture of our model space, although not as clear as in the three-slope case, is still informative. There is no hidden level of complexity. Therefore with the four-slope graph it is easy to define the excitations relative to a given determinant or to remove individually selected determinants, both tasks demanding some tricks when the orbital configurations are used. Moreover, the calculation of matrix elements using the four-slope graph is very simple and the structure of the model space may be used as effectively as in the previous case.

Although the number of different structures of two-, three- and four-segment loops is rather high in the present case—for example, each of the loops of figure 3, without doubly occupied arcs, come in six versions when α and β singles are differentiated—we may easily obtain the phases of matrix elements by assigning signs to the segments of a loop. Let t_i be the type of an arc i in a given path, i.e. $t_i = 0, \bar{1}, 1, 2$. The formula

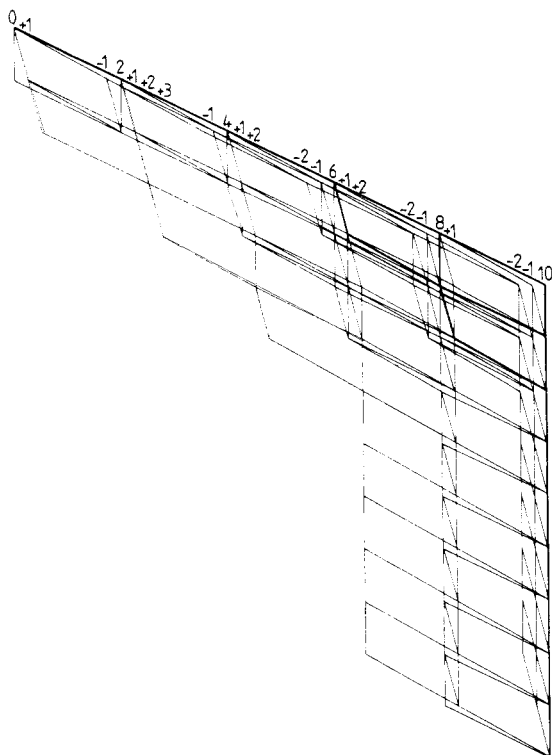


Figure 9. The graph of figure 1 as a four-slope graph.

for diagonal matrix elements now reads:

$$\begin{aligned} \langle L|H|L\rangle = & \sum_{i=1}^n n_i(i|i) + \sum_{i,j=1}^n \delta_{n,2}(\delta_{n,1} + \delta_{n,2})(2J_{ij} - K_{ij}) \\ & + \sum_{i<j=2}^n \delta_{n,1}\delta_{n,1}(J_{ij} - \delta_{i,t_j}K_{ij}). \end{aligned} \quad (10)$$

Consider now the case of one spin orbital different in each path, say j in L and i in R, $i < j$. The formula is

$$\begin{aligned} \langle L|H|R\rangle = & \varepsilon_{LR} \left((i|j) + \sum_{k=1}^n [n_k(ij|kk) - (\delta_{n,k} + \delta_{n,k}\delta_{i,t_j})(ik|jk)] \right) \\ \varepsilon_{LR} = & \prod_{p=i}^j \varepsilon_p \end{aligned} \quad (11)$$

where ε_p are signs defined for the loop segments (see table 2), and $n_k = \min(n_k^L, n_k^R)$.

Some subtleties arise if there are two different spin orbitals in each path. Let us say that orbitals $i < k$, belonging to L, are different from $j < l$ belonging to R. This time i, j, k, l levels are not necessarily in top-down sequence. The general formula is

$$\begin{aligned} \langle L|H|R\rangle = & \varepsilon_{LR}((ij|kl)\delta_{i,t_j}\delta_{i,t_l} - (il|jk)\delta_{i,t_l}\delta_{i,t_k}) \\ \varepsilon_{LR} = & \prod_{p=\min(i,j)}^{\max(k,l)} \varepsilon_p \end{aligned} \quad (12)$$

Table 2. Phase factors for the four-slope graph. Segments $|0\ 0\rangle$, $|2\ 2\rangle$, $|0\ 2\rangle$, $|2\ 0\rangle$, $|0\ \bar{1}\rangle$, $|\bar{1}\ 0\rangle$, $|0\ \bar{1}\rangle$, $|\bar{1}\ 0\rangle$: always +1. $\varepsilon(|\bar{1}\ \bar{1}\rangle) = \varepsilon(|\bar{1}\ \bar{1}\rangle) = \varepsilon(|\bar{1}\ \bar{1}\rangle) = \varepsilon(|\bar{1}\ \bar{1}\rangle)$, $\varepsilon(|\bar{1}\ 2\rangle) = -\varepsilon(|\bar{1}\ 2\rangle)$; $\varepsilon(|2\ \bar{1}\rangle) = -\varepsilon(|2\ \bar{1}\rangle)$.

Δe	-2	-1	0	1	2
$ \bar{1}\ \bar{1}\rangle$	+1	-1	+1	-1	+1
$ \bar{1}\ 2\rangle$	—	+1	-1	+1	-1
$ 2\ \bar{1}\rangle$	-1	+1	-1	+1	—

with ε_p signs given in table 2. Each loop consists of a maximum of four non-parallel segments. However, there are four segments that count as a double segment: $|2\ 0\rangle$, $|0\ 2\rangle$, $|\bar{1}\ \bar{1}\rangle$ and $|\bar{1}\ \bar{1}\rangle$. The second pair appear when the same orbital, but with a different spin function, appears in the opposite determinant. The loops involving these segments are of two- or three-segment type. For example, the off-diagonal parts of the formula (4) correspond to the loop type $|\bar{1}\ \bar{1}\rangle$.

Calculation of the whole matrix proceeds exactly in the same way as described in the previous sections. The loops giving non-zero elements are formed in the graph in some systematic manner; fixing one of the paths and making all other paths interact with it, or fixing the levels on which the non-parallel segments are placed, the levels corresponding to integral indices. In the second case the structure of the matrix may be effectively used to store it in a compact way.

7. D and E parts of the graph

In figures 1, 8 and 9 we see that the D and E parts of the graph have an especially simple structure. When these parts are large it is worthwhile to ask: how can we benefit from this simplicity? We have already noticed that fixing the levels corresponding to the integral indices we find a large number of matrix elements equal up to a phase (cf figure 4). This is true for the majority of matrix elements with L and R configurations differing by two orbitals; if they differ by one orbital only partial matrix elements can be formed and treated in the same way. For example, we may find all matrix elements in which an $(i|j)$ integral or a combination of $2(ij|kk) - (ik|jk)$ integrals appear. In any case we have one value of matrix element and a whole set $\{m_L, m_R\}$ of pairs of numbers-positions of this element in the matrix. Storing a matrix in such a form already saves us space. However, when the E or D part is particularly simple, one can devise a labelling scheme for the paths in such a way that the numbers m_L and m_R are regularly spaced in the set $\{m_L, m_R\}$.

To be more specific, consider the case of a three-slope graph with a large E part occupied by no more than two electrons. Let us number the external orbitals from 1 to n_E , and designate by L and R the internal part of the two paths making a loop. The paths passing through the E_0 vertex (cf figure 1) are fully characterised by their internal paths labels; those passing through E_1 or E_2 require, in addition, labels of the occupied external orbitals for a full description. The index vector may be defined separately for each vertex E_k using the recursive definition:

$$\begin{aligned}
 I_0(m_L) &= I_0(m_L) + d(M, s_L) & I_0(1') &= 0 \\
 I_1(m_L) &= I_1(m_L) + d(M, s_L + 1) \cdot n_E & I_1(1') &= K_0
 \end{aligned}$$

$$I_2^1(m_L) = I_2^1(m_L) + d(M, s_L) \cdot n_E \quad I_2^1(1') = K_1$$

$$I_2^2(m_L) = I_2^2(m_L) + d(M, s_L + 2) \binom{n_E}{2} \quad I_2^2(1') = K_2$$

where L' is the next accepted path after L , I_k is the index vector for the paths reaching the E_k vertex, and the two kinds of index vectors for the E_2 vertex are for the paths with one external double (I_2^1) and two external singles (I_2^2). Each index vector has as its lowest value (i.e. for the first accepted path, designated by $1'$) the total number of paths already numbered. For example, K_2 is equal to the number of paths crossing E_0 , E_1 and E_2 with one external double. Using these index vectors we can calculate the addresses $A(L; \dots)$ of the groups of determinants associated with a given configuration $(L; \dots)$:

$$A(L) = I_0(m_L)$$

$$A(L; a) = I_1(m_L) + (a - 1)d(M, s_L + 1)$$

$$A(L; a, a) = I_2^1(m_L) + (a - 1)d(M, s_L)$$

$$A(L; a, b) = I_2^2(m_L) + \left[\binom{\max(a, b) - 1}{2} + \min(a, b) - 1 \right] d(M, s_L + 2).$$

This addressing scheme groups together all determinants differing only in the external orbitals. Elements of the type $\langle L; a|H|R; a \rangle$ are now represented in a very compact way by giving first a block $d(M, s_L + 1)$ by $d(M, s_R + 1)$ of matrix elements, and a set of internal space contributions $\{I_1(m_L), I_1(m_R)\}$ to the final addresses of this block in the H matrix. If the number of $\{L, R\}$ pairs is K and there are D non-zero matrix elements in the block, $K + D$ computer words are used to represent $Kn_E D$ elements. Similar or even greater savings can be made for the case of elements $\langle L; aa|H|R; aa \rangle$ and $\langle L; a, b|H|R; a, b \rangle$.

Suppose now that the loop is formed entirely in the external part, i.e. matrix elements are of the $\langle L; a, b|H|L; c, d \rangle$ type. This time we may calculate the external part contribution to the addresses and run over all internal paths L joining the E_2 vertex, calculating $I_2^2(m_L)$. The structure of the matrix element block depends only on the value of s_L in this case. Therefore it is convenient to calculate the I_2^2 index vector in such a way that the internal path contributions for the paths with a fixed number of singles come consecutively.

In the mixed cases, when one, two or three loop levels belong to the external, and the remaining loop levels to the internal part of the graph, it is rather hard to get the I-part contributions with regular spacings. Then only the E part can be used efficiently. Most of the elements with one external loop index are of the type $\langle L; a, b|H|R; b \rangle$. The structure of this type of matrix element depends on s_L , s_R and the relation between a and b , but not on the value of b . Spin paths corresponding to the configuration $(L; a, b)$ with $a < b$, $a = b$ and $a > b$ differ; when b is lowered until $a < b$ is changed to $a > b$ the spin functions with $(++)$ or $(--)$ as the last two segments are not affected, but those with $(+-)$ are changed to $(-+)$ and vice versa. Due to the nature of lexical ordering of the spin paths, first come the $d(M + 2, s_L)$ functions with the last two segments $(--)$, then $d(M, s_L)$ with $(+-)$, $d(M, s_L)$ with $(-+)$ and the last $d(M - 2, s_L)$ functions with $(++)$, so that rows $d(M + 2, s_L) + 1$ to $d(M + 2, s_L) + d(M, s_L)$ are changed with rows $d(M + 2, s_L) + d(M, s_L) + 1$ to $d(M + 2, s_L) + 2d(M, s_L)$ when b

becomes lower than a . Again, from one block with D non-zero matrix elements, and a set of K pairs $\{L, R\}$, we obtain $Kn_E D$ elements.

In the case of two external indices in a loop most elements are of the $\langle L; a, c | H | R; b, c \rangle$ type, $a > b$. Here inequalities $c > a, b; a > c > b; a, b > c$ lead, similarly to the previous case, to the reordering of columns and rows inside the $d(M, s_L + 2)$ by $d(M, s_R + 2)$ dimensional block of matrix elements. Moreover, two kinds of loops (figures 3(a) and (b)) are easily taken into account by taking the $\langle L; b, c | H | R; a, c \rangle$ element. Unfortunately a compact representation of the numerous $\langle L; a, b | H | R; c \rangle$ matrix elements is rather difficult, but even here, depending on the position of the loop segment in the I part, the internal contributions from $\{L, R\}$ change in a rather regular way.

It is clear that the graphical representation not only allows for the rapid evaluation of matrix elements, but also gives us an insight into the structure of the matrix reflecting the structure of the model space described by a graph, so that the whole matrix representative of an operator is represented in this space in a very compact form. The 'seed' matrix element blocks are placed in the proper places in the final matrix by a small routine recreating the addresses of the configuration pairs. When the three-slope graph is used there is a degree of freedom associated with the order of spin paths, i.e. the order of determinants connected with an orbital configuration, and, using the index vector, also in the order of internal contributions to the path addresses. The two-level addressing described here may not be optimal in some cases—more complicated three-level addressing schemes, with separate addressing in the D, A and E parts, may then be used. Elaboration of details is rather straightforward and depends on the particular method of calculation we want to use.

8. Summary

In this paper I have tried to introduce in a simple way some concepts related to the graphical representation of the many-electron model spaces with determinants used as basis functions. My intention was to indicate possibilities rather than to exhaust the subject: not only are other graphical representations of determinants possible, but graphs representing eigenfunctions of spin or angular momentum operator eigenfunctions were also found to be useful (Duch 1985). For pedagogical reasons it is convenient to first introduce the simplest, two-slope graph, shown in figure 1. Such a graph was recently used in relativistic configuration–interaction calculations (Esser 1984). However, if M is a good quantum number the graph has to be changed. The simplest modification involves separation of α - and β -type spin orbitals, as shown in figure 5. This arrangement was used by Wasilewski in his configuration–interaction (CI) program (Wasilewski 1984). It is also implicit in the paper by Knowles and Handy (1984) on the full CI method, although, due to the high symmetry of a full space, the explicit graphical representation was not used. Representation of a restricted model space by the two-slope graphs is not as flexible as by the three- and four-slope graphs. The n -level, three-slope graph, describing orbital configurations, was introduced as a side projection of a three-dimensional graph (figure 7). The three-slope graph is particularly convenient for the visualisation of the model spaces (figure 8), hiding some of the three-dimensional graph complexity. With each configuration we can associate a group of basis functions (determinants in this case); functions within that group are classified using the M diagram (figure 6). Graphs describing orbital configurations were used

previously (Duch and Karwowski 1982) in connection with the branching diagram (Pauncz 1979) to describe the basis of spin eigenfunctions.

The four-slope graph (figure 9), on the other hand, does not 'hide' anything, being an oblique projection of the three-dimensional graph. The calculation of matrix elements is still simple, although the graph itself is rather complex: loop segments are counted to find the sign (table 2) while the integral indices are given by that level in which the two arcs of a loop segment are not identical. Similar four-slope graphs are used in the graphical unitary group approach (Shavitt 1977a, 1978, 1983) for a description of spin eigenfunctions (Gelfand basis). Indeed, removing vertices corresponding to $M < 0$ values from our four-slope graph we would obtain the Shavitt graph.

More complicated graphs, with the symmetry-split vertices or different number of slopes at each level, may still be useful. However, one should avoid excessive complication using either suitably projected graphs or using such technical devices as the index vector for selection of the paths. Although fairly flexible selection of configurations is possible, the efficiency of a graphical matrix element calculation favours longer, but more 'natural' bases (from the point of view of a graph). For example, leaving all determinants described by the graphs in figures 8 and 9, instead of selecting only those which are no more than doubly excited relatively to the three references paths, improves the efficiency of matrix element calculation and adds the most important higher excited determinants to our basis. If the complete active space method (Roos *et al* 1980) is followed by the configuration-interaction calculations the graph is composed from a large external part attached to the internal part corresponding to the full model space with a small number of orbitals—a very good example of the 'natural' basis from the graphical point of view.

The wide range of applications and a potential for further development makes the graphical representation of model spaces a useful tool in large-scale atomic and molecular calculations.

Acknowledgments

I wish to thank J Karwowski, J Wasilewski and W Nowak for many discussions and their comments on the manuscript. Support by the Institute for Low Temperature Research, Polish Academy of Science, contract no MR.I.9, is gratefully acknowledged.

Appendix 1. Computer representation of a graph

The most straightforward way to represent a p -slope graph is to use a matrix of dimension n by $N(p+1)$, each vertex represented by its weight and the weights of p arcs off this vertex. It is not hard to find a more economical way to represent a graph. Let us take the three-slope graph of figure 8 as an example. It has $V = 45$ vertices that we can number from the top down and from left to right in each row. Then a vertex (i, j) has a number $v_{ij} = B(i) + j$, calculated with the help of an auxiliary array $B(i)$. In our example:

$$B = [1, 2, 3, 4, 6, 9, 13, 16, 19, 22, 25, 28, 31, 34, 35].$$

We can represent the graph by three vectors (or, in general, p vectors) each of length V , such that $y_k(v_{ij})$, $k = 0, 1, 2$, gives the weight of the k -fold occupied arc. At

each row i the v_{ij} numbers change from $v_{ij} = B(i) + J_{\min}(i)$ to $v_{ij} = B(i) + J_{\max}(i)$. The values of J_{\min} and J_{\max} are also stored:

$$J_{\min} = [0, 0, 2, 4, 5, 6, 7, 8, 8, 8, 8, 8, 8, 8, 10]$$

$$J_{\max} = [0, 2, 4, 6, 8, 10, 10, 10, 10, 10, 10, 10, 10, 10, 10].$$

The y_1 and y_2 vectors contain the arc weights of singly and doubly occupied arcs. A negative value of the arc weight means that this arc does not belong to the graph. The y_0 vector is a special case, because all arc weights of the empty arcs are zero. Therefore we need it only to flag the arcs that are removed. Let $y_0(v_{ij}) = \pm w_{ij}$, i.e. plus or minus the weight of the v_{ij} vertex, where 'plus' is taken when the empty arc off v_{ij} vertex belongs to the graph and 'minus' when it does not. If we want to remove a vertex v_{ij} that is inside the graph, i.e. $J_{\min}(i) < j < J_{\max}(i)$, we simply put $y_0(v_{ij}) = 0$.

The three auxiliary arrays B , J_{\min} , J_{\max} (n -dimensional each) and the three vectors y_0 , y_1 , y_2 (V -dimensional each) give a very economical and convenient computer representation of a graph. In our example the y_k vectors are

$$y_0 = [1, -1, -1, 1, -3, -2, 1, -6, 3, 1, -9, 10, 4, 1, -19,$$

$$23, 15, 5, 1, -42, 57, 43, 21, 99, 142, 121, 99, 241, 362, 99,$$

$$340, 702, 99, 439, 1141, 99, 538, 1679, 99, 637, 2316, -99, -736, 3052, -3887]$$

$$y_1 = [0, -1, 1, 0, -1, 1, 0, 3, 1, 0, 10, 4, 1, 0, 23,$$

$$15, 5, 1, -1, 57, 43, 21, -1, 142, 121, -1, 241, 362, -1, 340,$$

$$702, -1, 439, 1141, -1, 538, 1679, -1, 637, 2316, -1, -1, 3052, -1, -1]$$

$$y_2 = [0, 2, 1, 0, 3, 1, 0, 4, 1, 0, 14, 5, 1, 0, 38,$$

$$20, 6, -1, -1, 100, 64, -1, -1, 263, -1, -1, 603, -1, -1, 1042,$$

$$-1, -1, 1580, -1, -1, 2217, -1, -1, 2953, -1, -1, 3788, -1, -1, -1].$$

Appendix 2. Searching paths in a graph

An algorithm to calculate efficiently the lexical indices of the paths connecting two given vertices in a graph is of fundamental importance if the matrix elements are calculated with the help of a graph. The literature on searching the general graphs is extensive (cf Knuth 1973). However, in the case of the p -slope graphs one can find more specific and therefore more effective methods to search the paths. Two classes of such methods may be distinguished: depth search and breadth search.

Depth search methods generate the paths one by one; it is natural to represent the paths as an array of arcs (or rather, arc types) in this context. Let us take as an example the three-slope graph case and suppose that we have two vertices: $A = (n_a, N_a)$ and $B = (n_b, N_b)$, $n_a < n_b$ and $N_a \leq N_b$ (in the case of a four-slope graph the M_a, M_b values are needed in addition). $\Delta n = n_b - n_a$ arcs should accommodate $\Delta N = N_b - N_a$ electrons. The rightmost path is easy to find: it has $k_2 = \text{Int}(\Delta N/2)$ doubles, where Int takes an integer part of a number, and $k_1 = \Delta N - 2k_2$ singles (at least, because the number of singles $k_1 \geq 2M$), the rest, i.e. $k_0 = \Delta n - k_1 - k_2$, being empty arcs. Each vertex on a path connecting A and B is characterised by a triple $[k'_0, k'_1, k'_2]$, at A equal to $[k_0, k_1, k_2]$ and at B equal to $[0, 0, 0]$. Moving from A to the next vertex we have $[k_0, k_1, k_2 - 1]$

if we move through the doubly occupied arc, $[k_0, k_1 - 1, k_2]$ if through single, and $[k_0 - 1, k_1, k_2]$ if through unoccupied. Of course we have to check each time if the new vertex belongs to the graph and if the new k_0, k_1, k_2 are not negative. Each time we reach B we move back up to the vertex where a new branching is possible. A very simple example will illustrate this procedure. Let $k_0 = k_1 = k_2 = 1$ at the vertex A ; the rightmost path is then 210 and the triples for the vertices belonging to this paths are: $[k_0, k_1, k_2] = [1, 1, 1], [1, 1, 0], [1, 0, 0], [0, 0, 0]$. From B we move back by two arcs (occupations) to the vertex with $[1, 1, 0]$ and this time decrease k_0 instead of k_1 , so that the $[1, 1, 0], [0, 1, 0], [0, 0, 0]$ sequence follows, corresponding to 201 occupations. The last two occupations form the leftmost path, so we back up by three occupations to A and decrease k_1 instead of k_2 obtaining $[1, 0, 1]$ triple, decrease now k_2 to get $[1, 0, 0], [0, 0, 0]$, i.e. occupations 120. Moving up by two occupations to $[1, 0, 1]$ and down to $[0, 0, 1], [0, 0, 0]$ we get path 102; up to $[1, 1, 1]$, which is reached by increasing k_1 we decrease k_0 to get two more paths: 021 and 012. Finally we take $k_1 = k_1 + 2$ and $k_0 = k_0 - 1, k_2 = k_2 - 1$: $[k_1, k_2, k_3] = [0, 3, 0]$, giving the 111 path. This algorithm finds the paths with fixed number of singles, which is sometimes an advantage. We may store not only $[k_0, k_1, k_2]$ triples at each intermediate vertex, but also sums of arc weights, etc, so that backing up to a level i' and then branching down partial results calculated down to level i' are used. One may define this algorithm recursively in an elegant way but it is better to avoid recursion in actual programming.

The breadth search algorithms, being non-recursive, are somehow easier to describe. At each level between n_a and n_b one pass is made over the vertices and the arc weights are added to the appropriate partial lexical numbers. The leftmost and the rightmost paths are easily found; for each level $n_a \leq k \leq n_b$ they give us the leftmost vertex $v_l(k)$ and the rightmost vertex $v_r(k)$ through which the paths connecting A with B may pass. For each vertex between $v_l(k)$ and $v_r(k)$ we form a stack of partial lexical paths numbers. At level $n_a + 1$ these numbers are equal to the weights of arcs leading to $v_l(n_a + 1), \dots, v_r(n_a + 1)$. To find the contributions from arcs between a level k and $k + 1$ we simply add all partial lexical paths numbers from a stack corresponding to the vertex $v_{kN'}, v_l(k) \leq v_{kN'} \leq v_r(k)$, increased by the weight of an arc joining $v_{kN'}$ vertex with a vertex $v_{k+1N'}$, to the stack of the $v_{k+1N'}$ vertex, for all (at most p) $v_{k+1N'}$ vertices, $v_l(k + 1) \leq v_{k+1N'} \leq v_r(k + 1)$ connected with $v_{kN'}$. Moving systematically from $k = n_a, \dots, n_b - 1$ and for each k from $v_{kN'} = v_l(k), \dots, v_r(k)$ we obtain as a result a set of lexical indices, ordered from the highest to the lowest, of the paths joining the A and B vertices.

A number of more specialised search algorithms could be formulated, for example for full model spaces or one reference case, but we shall not describe them here. It is worth noticing that, given a lexical index m_L of a path terminating at some vertex B and starting at the head of the graph, it is very easy to find this path. The weights of the arcs connected to B from above decrease with increasing slope. The last arc of path L is the one with the maximum weight $w \leq m_L$. We now take $m_{L'} = m_L - w$ and move to the new vertex via this arc, finding the maximum weight $w' \leq m_{L'}$ and repeating this procedure until we reach the head of the graph.

References

- Duch W 1985 *Lecture Notes in Chemistry* (Berlin: Springer) to be published
 Duch W and Karwowski J 1982 *Int. J. Quantum Chem.* **22** 783

- Esser M 1984 *Int. J. Quantum Chem.* **26** 313
- Hausman R F and Bender C F 1977 *Methods of Electronic Structure Theory* ed H F Schaefer (New York: Plenum) p 277
- Karwowski J 1973 *Theor. Chim. Acta* **29** 151
- Knowles P J and Handy N C 1984 *Chem. Phys. Lett.* **111** 315
- Knuth D E 1973 *Sorting and Searching. The Art of Computer Programming* vol 3 (Reading, MA: Addison-Wesley)
- Paldus J 1976 *Theoretical Chemistry: Advances and Perspectives* vol 3, ed H Eyring and D J Henderson (New York: Academic) p 131
- Pauncz R 1979 *Spin Eigenfunctions: Construction and Use* (New York: Plenum)
- Roos B O 1972 *Chem. Phys. Lett.* **15** 153
- Roos B O and Siegbahn P E M 1977 *Methods of Electronic Structure Theory* ed H F Schaefer (New York: Plenum) p 277
- Roos B O, Taylor P R and Siegbahn P E M 1980 *Chem. Phys.* **48** 157
- Saunders V R and van Lenthe J H 1983 *Mol. Phys.* **48** 923
- Shavitt I 1977a *Int. J. Quantum Chem.* **S11** 131
- 1977b *Modern Theoretical Chemistry* vol 3, ed H F Schaefer (New York: Plenum) p 189
- 1978 *Int. J. Quantum Chem.* **S12** 5
- 1983 *New Horizons of Quantum Chemistry* ed P-O Löwdin and B Pullman (Dordrecht: D Reidel) p 279
- Slater J C 1968 *Quantum Theory of Matter* 2nd edn (New York: McGraw-Hill)
- Wasilewski J 1984 Private communication